

## LIGHT-ION SCATTERING

### MEASUREMENTS OF $X_2$ AND OTHER RESULTS IN THE ANALYSIS OF $d + {}^{58}\text{Ni}$ ELASTIC SCATTERING

E.J. Stephenson, J.C. Collins, C.C. Foster, D.L. Friesel, J.R. Hall, W.W. Jacobs,  
W.P. Jones, M.D. Kaitchuck, and P. Schwandt  
Indiana University Cyclotron Facility, Bloomington, Indiana 47405

W.W. Daehnick  
University of Pittsburgh, Pittsburgh, Pennsylvania 15260

During 1981, measurements have been completed of the tensor analyzing powers  $A_{yy}$  and  $X_2 = (2A_{xx} + A_{yy})/\sqrt{3}$  in the elastic scattering of 80 MeV deuterons from  ${}^{58}\text{Ni}$ . All of the elastic scattering measurements, including the cross section and vector analyzing power  $A_y$ , are shown in Fig. 1. The new measurements of  $A_{yy}$  are large near  $21^\circ$ , showing an effect of interference that is also prominent in  $A_y$ . The measurements of  $X_2$  were made on a special scattering table set at  $54.7^\circ$  to the horizontal plane (described in Ref. 1). To first order,  $X_2$  does not depend on spin-orbit forces,<sup>2</sup> and is expected to be a sensitive test of the presence of tensor potentials between the deuteron and the nucleus.<sup>3</sup> The measurements of  $X_2$  show little structure, and are about half the size of measurements at 56 MeV.<sup>4</sup> At large angles they are much smaller than the predictions of Ref. 3.

While most of the general features of the data shown in Fig. 1 can be reproduced with global optical potential calculations,<sup>5</sup> significant improvements can be made if the potential parameters are adjusted. It was found that the use of a squared Woods-Saxon form for the radial dependence of the real central potential was significantly better than a Woods-Saxon form. This led to the use of an "arbitrary" shape composed of a series of Gaussian functions added to the traditional potential.<sup>6</sup> The spacing of the

Gaussians was chosen to match the deuteron wavelength, and their width was chosen to minimize oscillations in their sum. Only the strengths were varied to improve agreement between the calculation and the data. The resulting calculation is a compromise that favors good reproduction of the cross section and vector analyzing power (the solid curve in Fig. 1). The cross section minima and large angle slope are well-reproduced, as is the pattern of the oscillations in  $A_y$ . The large  $A_{yy}$  values near  $21^\circ$  are reproduced, but the calculation overestimates the oscillatory pattern at larger angles. No tensor potentials were included in this fit, and the structures in  $X_2$ , which depend to first order on those terms, are not reproduced.

The "arbitrary" potential is depicted in Fig. 2 by the cross-hatched bands corresponding to one-standard-deviation errors in the potential. The width of the bands was computed from the diagonal elements of the error matrix of the fit. (Although correlation coefficients were not large, they may alter the error band in a complete calculation.) The solid curve is a "best-fit" potential using traditional radial shapes.<sup>5</sup> There are significant differences. The real central potential is more shallow in the surface and deeper in the interior. The imaginary and spin-orbit parts seem well-reproduced by the traditional shapes. The data determine the real parts of the

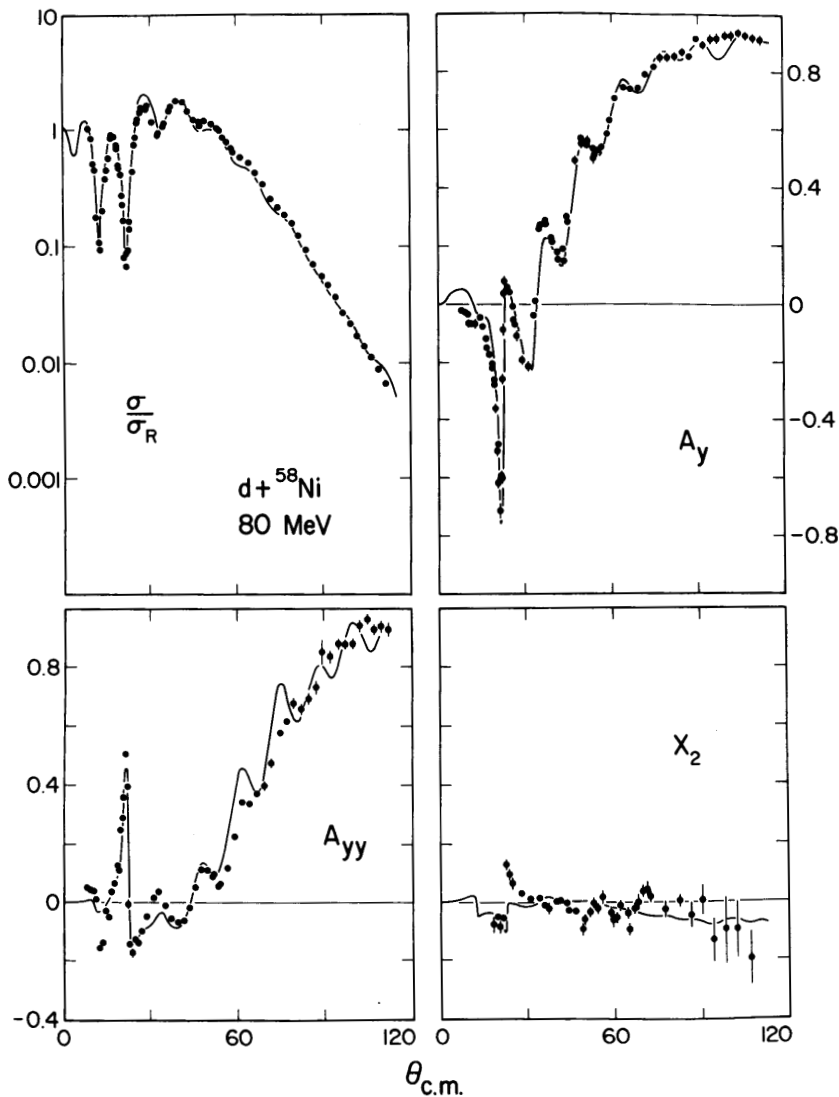


Figure 1. Measurements of the cross section (ratio to Rutherford), vector ( $A_y$ ), and tensor ( $A_{yy}$  and  $X_2$ ) analyzing powers for 80 MeV deuterons elastically scattered from  $^{58}\text{Ni}$ . The optical model calculations employ the "arbitrary" potential displayed in Fig. 2.

potential to a much higher precision than the imaginary parts. This is an artifact of rainbow scattering, in which the real parts of the potential play a dominant role.

Most analyses<sup>4</sup> of the effects of tensor potentials in deuteron elastic scattering have found that the  $T_R$  potential is predominantly imaginary. Adding such a potential to our calculation (with half the strength) serves to reproduce some of the diffractive structure of the

measurements of  $X_2$  (see Fig. 3). Contrary to experience at lower energies, such a potential has a profound effect on other analyzing powers. The vector analyzing power has no values larger than 0.8 and the  $A_{yy}$  tensor analyzing power is noticeably reduced in magnitude. These differences occur primarily in the region beyond the rainbow angle, in a range of momentum transfer not seen in lower energy measurements.

It has been previously reported that microscopic

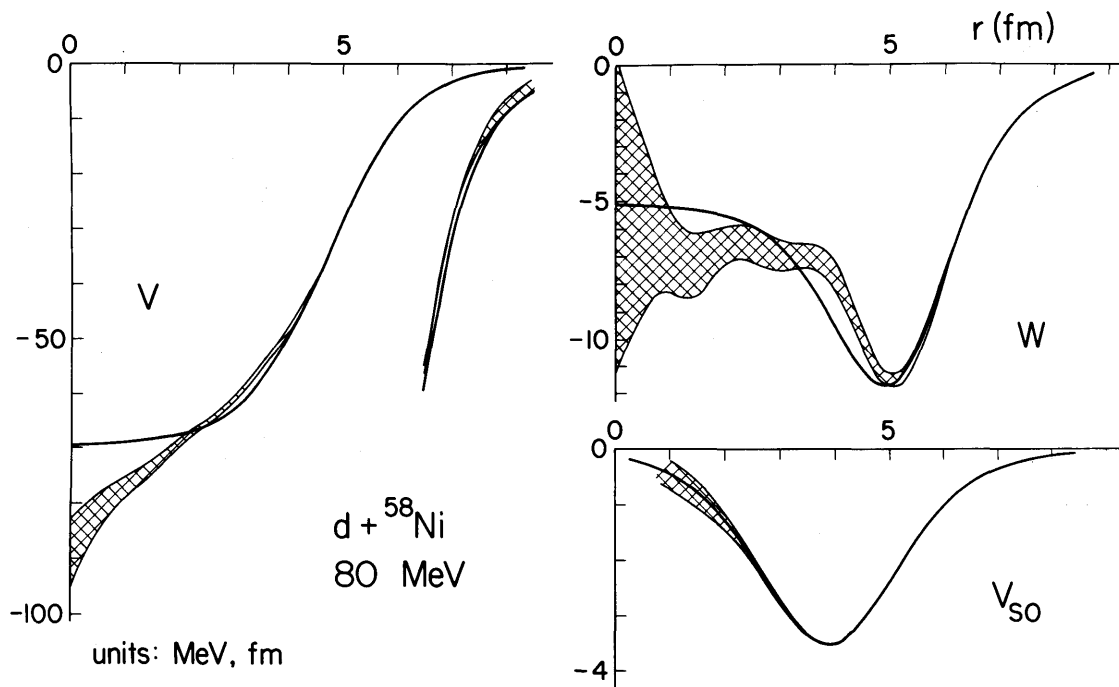


Figure 2. Comparison between the "best-fit" potential using traditional radial shapes (solid line), and the error band associated with an "arbitrary" potential. Beyond 6.5 fm, the real central potentials are multiplied by 10 to make the differences visible.

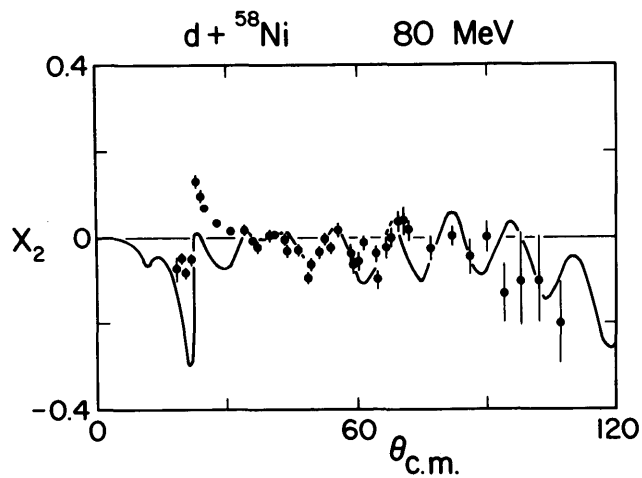


Figure 3. Measurements of  $X_2$  and an optical model calculation including a  $T_R$  potential of half the strength of the one reported in Ref. 4.

calculations of deuteron elastic scattering that include coupling to break-up states<sup>7</sup> provide a surprisingly precise reproduction of the measurements.<sup>1</sup> The calculations for  $X_2$  are shown in Fig. 4. They are in general agreement with the measurements and tend to support the microscopic calculation. Figure 4 also contains predictions for  $A_{xz}$ , which may be measured if the quantization axis of the polarized deuteron beam is placed in the scattering plane at  $45^\circ$  to the beam momentum. Unlike  $X_2$ , large differences are seen between the predictions of the microscopic model and the optical model, with or without tensor (in this case, the  $T_R$  potential from Ref. 3 is purely real). Measurements of  $A_{xz}$  that followed the solid curve would constitute evidence that the optical model is incapable of successfully reproducing deuteron elastic scattering data.

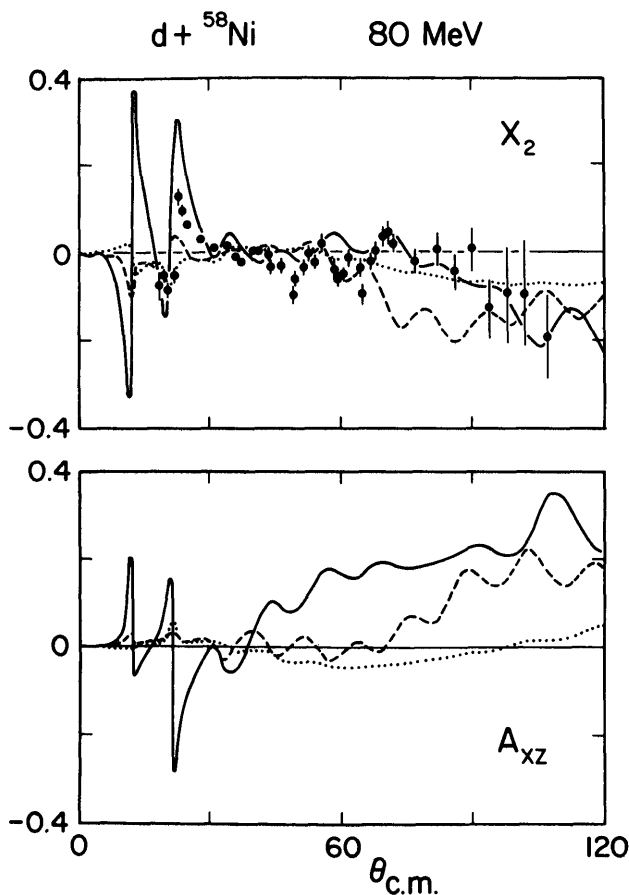


Figure 4. Measurements of  $X_2$  and calculations of  $X_2$  and  $A_{xz}$  using a microscopic model of Ref. 7 (solid curve) and an optical model with and without (dashed and dotted) the real  $T_R$  potential of Ref. 3.

MEASUREMENT OF THE RELATIVE SIGN OF NEUTRON ( $M_n$ ) AND PROTON ( $M_p$ ) TRANSITION MATRIX ELEMENTS FOR THE  $2^+_2$  STATE IN <sup>30</sup>Si BY INELASTIC ALPHA-PARTICLE SCATTERING.

A. Saha, K.K. Seth and D. Barlow  
Northwestern University, Evanston, Illinois 60201

H. Nann and W.W. Jacobs  
Indiana University Cyclotron Facility, Bloomington, Indiana 47405

One of the most exciting recent developments in the study of nuclear structure has been the appreciation of the isovector characteristics of nuclear excitation. A number of different experimental techniques have been developed to examine the separate roles played by neutrons and protons in the nuclear

- 1) C.C. Foster, J.C. Collins, D.L. Friesel, J.R. Hall, W.W. Jacobs, W.P. Jones, M.D. Kaitchuck, P. Schwandt, E.J. Stephenson, and W.W. Daehnick, IUCF Scientific and Technical Report 1980, p. 71.
- 2) D.J. Hooton and R.C. Johnson, Nucl. Phys. A175, 583 (1971); R.C. Johnson, Nucl. Phys. A293, 92 (1977).
- 3) E.J. Stephenson, C.C. Foster, P. Schwandt, and D.A. Goldberg, Nucl. Phys. A359, 316 (1981).
- 4) K. Hatanaka, M. Nakamura, K. Imai, T. Noro, H. Shimizu, H. Sakamoto, J. Shirai, T. Matsusue, and K. Nisimura, Polarization Phenomena in Nuclear Physics - 1980 (AIP Conf. Proc. No. 69) p. 478.
- 5) W.W. Daehnick, J.D. Childs, and Z. Vrcelj, Phys. Rev. C 21, 2253 (1980).
- 6) I. Brissaud and M.K. Brussel, J. Phys. G. 3, 481 (1977).
- 7) G.H. Rawitscher and S.N. Mukherjee, Nucl. Phys. A342, 90 (1980).

excitations. In inelastic scattering, the cross section for the transition to an excited state can be described in terms of separate matrix elements for proton and neutron excitations,  $M_p$  and  $M_n$ , respectively, or in terms of isoscalar and isovector matrix elements,  $M_0 = M_n + M_p$  and  $M_1 = M_n - M_p$ . The cross